

## Phase Separation of Aqueous Solutions of Poly(*N*-isopropylacrylamide) Investigated by Confocal Raman Microscopy

Yasushi Maeda,\* Hiroki Yamamoto, and Isao Ikeda

Department of Applied Chemistry and Biotechnology,  
Fukui University, Fukui 910-8507, Japan

Received March 12, 2003

Revised Manuscript Received May 25, 2003

**Introduction.** Aqueous solutions of poly(*N*-isopropylacrylamide) (PiPA) exhibit a phase separation above ca. 32 °C. The phenomenon has been investigated various kinds of methods including turbidimetry,<sup>1</sup> calorimetry,<sup>2</sup> NMR,<sup>3</sup> fluorescence,<sup>4</sup> light scattering,<sup>5</sup> neutron scattering,<sup>6</sup> IR spectroscopy,<sup>7</sup> and Raman spectroscopy.<sup>8</sup> These studies have revealed that the macroscopic phase separation or clouding of the solutions is accompanied by changes in conformation and hydration state of polymer chains. Raman spectroscopy provides information about molecular vibrations, which are sensitive to interactions and conformations of the molecules. Its spatial resolution can be better than 1  $\mu\text{m}$  in the lateral plane by focusing laser beam on the samples. Moreover, when confocal optics is utilized, which is equipped with a pinhole placed in the back focal plane of the microscope, the spatial resolution along the vertical direction is as good as in the lateral direction. Therefore, confocal Raman microscopy has been used to study the distribution of components inside various materials such as binary mixtures of polymers<sup>9</sup> and aqueous polymer gels.<sup>8b,c</sup> In this study, we use confocal Raman microscopy to investigate phase separation of aqueous solutions of PiPA and poly(*N,N*-diethylacrylamide) (PDEA). Changes in the distribution of the polymers and additives in the aqueous two-phase systems are discussed.

**Experimental Section.** Methods of preparation of PiPA ( $M_w = 11\,000$ ) and PDEA ( $M_w = 19\,000$ ) have been described elsewhere.<sup>7,10</sup> Raman spectra were measured using a NRS-1000 micro-Raman spectrometer (JASCO, Japan) equipped with an Ar laser (GLG2169, Showa Optronics, Japan) and an electronically cooled (−80 °C) CCD detector (DU401FI, Andor, 1024  $\times$  128 pixel). The Ar laser was operated at 514.5 nm, and the spectra were collected at a resolution of ca. 1  $\text{cm}^{-1}$ . A pinhole aperture (50  $\mu\text{m}$ ) and a 50 $\times$  objective lens give a spatial resolution of ca. 2 and 4  $\mu\text{m}$  to the lateral and vertical direction of the sample, respectively. A sample solution was placed between a holed slide glass and a cover glass and put on a metal block thermostated by circulating water bath. Point-by-point mapping was carried out using a motorized scanning stage controlled by computer software. For the formation of a two-dimensional molecular map of the sample, an area of 30  $\mu\text{m} \times 30 \mu\text{m}$  with the point distance of 1  $\mu\text{m}$  was measured.

**Results and Discussion.** The course of the phase separation of aqueous solution of PiPA can be observed by optical microscopy. Particles that appeared at ca. 32

°C underwent Brownian motion, increased in size by aggregation, and finally adsorbed on the surface of the glass. The optical microscopic image of the aqueous two-phase system of PiPA at 40 °C is shown in Figure 1a. Raman spectra measured at the points in the domain and matrix phases of the system are shown in Figure 1c. The C–H stretching vibration ( $\nu(\text{C–H})$ ) band observed between 2800 and 3000  $\text{cm}^{-1}$  indicates the presence of PiPA. The domain is rich in polymer, but the matrix also contains a small amount of polymer. Moreover, the  $\nu(\text{C–H})$  band for the methylene groups of the main chain appears at a lower wavenumber in the polymer-rich phase (2924  $\text{cm}^{-1}$  at 40 °C) than in the solvent-rich phase (2944  $\text{cm}^{-1}$  at 40 °C) and in the single-phase solution (2943  $\text{cm}^{-1}$  at 30 °C). Because the position of the band in neat solid PiPA is 2922  $\text{cm}^{-1}$  and, in general, a C–H stretching band undergoes a blue shift upon interaction with water,<sup>11</sup> the result suggests that the main chain is partially dehydrated in the polymer-rich phase. The integrated intensity ratio of the  $\nu(\text{C–H})$  band of PiPA to the O–H stretching vibration band of water ( $A_{\text{C–H}}/A_{\text{O–H}}$ ) was used to acquire a two-dimensional molecular map in the area of 30  $\times$  30  $\mu\text{m}$  (Figure 1b), which is indicated with the square in the photographic image. The distribution of the polymer was not completely homogeneous within the droplet because there are small pools of the solvent-rich phase inside the droplet.

Next, we measured Raman spectra at different PiPA concentrations ( $W_p$ , wt %) below the lower critical solution temperature (LCST) (20 °C) to know the relationship between  $A_{\text{C–H}}/A_{\text{O–H}}$  and  $W_p$ . As expected,  $A_{\text{C–H}}/A_{\text{O–H}}$  is proportional to  $W_p/(100 - W_p)$  (Figure 2). If we ignore the effects of temperature, we can obtain a first approximation of PiPA concentration in the phase-separated systems using the relationship as a calibration curve. The concentration of PiPA in the polymer-rich and solvent-rich phases at 40 °C and different overall polymer concentration is shown in Figure 2b. The concentration of PiPA in the polymer-rich phase and solvent-rich matrix is 51 and 9 wt %, respectively, when 10 wt % PiPA solution is phase-separated. Polymer concentrations in both phases gradually increase with an increase in the overall polymer concentration.

Next, we followed the compositional change in a selected droplet at a cooling process. Droplets kept their sizes at cooling and suddenly burst out at a temperature just below the LCST. Therefore, Raman measurement was easier during cooling than heating. As shown in Figure 3a, a sharp change in polymer concentration occurs in a narrow temperature range around 34 °C. On the other hand, PDEA exhibits a gradual change in the temperature range between 45 and 31 °C. The temperature range where change in polymer concentration occurs is coincident with the endothermic peak of DSC trace of each polymer (Figure 3b).

This method can also be used to reveal the distribution of additives such as cosolvents. Figure 4a shows Raman spectrum of the PiPA/H<sub>2</sub>O/2-propanol-*d*<sub>8</sub> ternary mixture in the  $\nu(\text{O–H})$  (3800–3100  $\text{cm}^{-1}$ ),  $\nu(\text{C–H})$  (3000–2800  $\text{cm}^{-1}$ ), and  $\nu(\text{C–D})$  (2300–2000  $\text{cm}^{-1}$ ) region. The concentrations of PiPA, H<sub>2</sub>O, and 2-propanol-*d*<sub>8</sub> can be estimated from the integrated intensities of

\* Corresponding author: Fax +81-776-27-8747; e-mail y\_maeda@acbio.fukui-u.ac.jp.

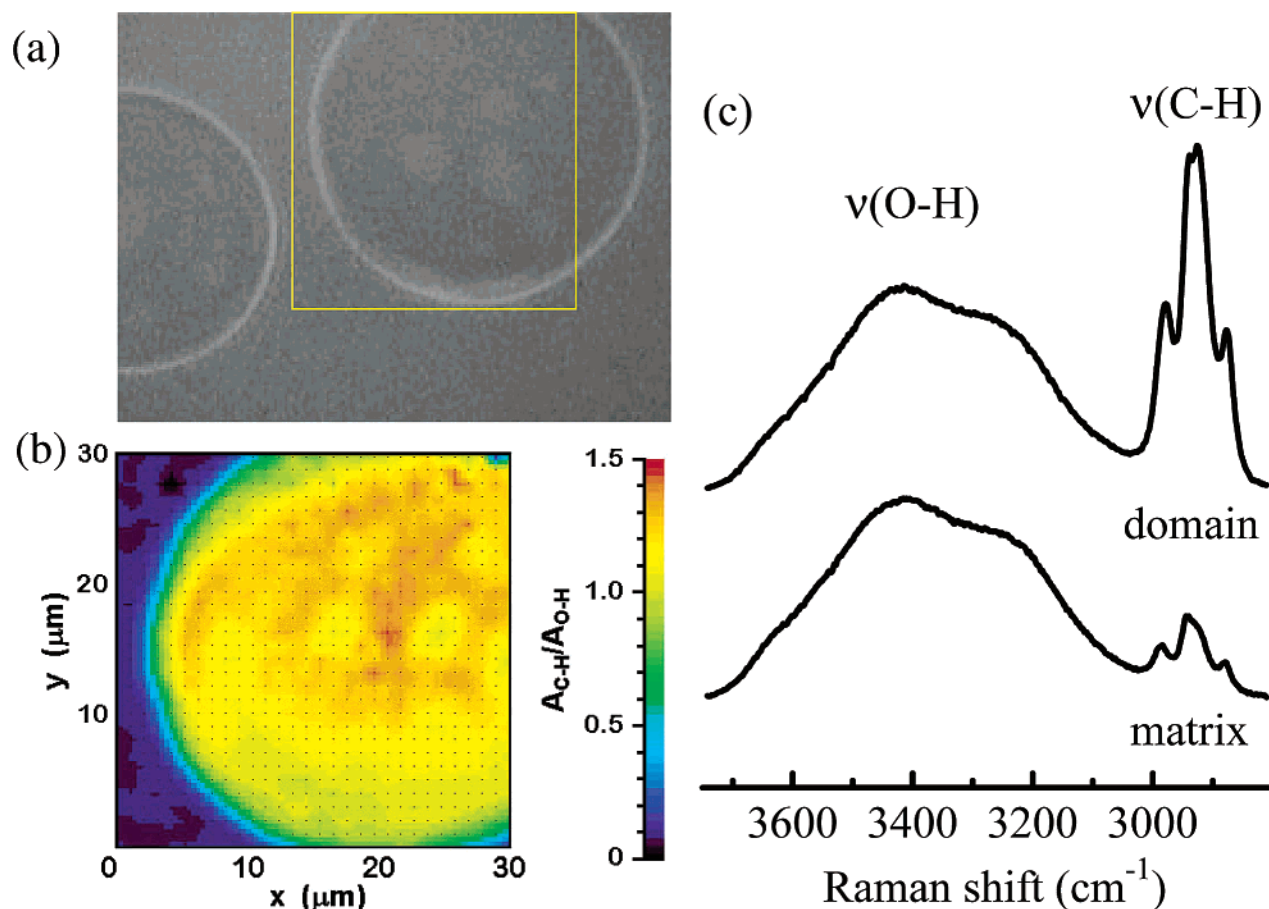


**Figure 1.** (a) Optical microscopic image of the droplets formed in 50 wt % PiPA/H<sub>2</sub>O at 40 °C. (b) Micro-Raman confocal image of the solution at the yellow square in (a). (c) Raman spectra measured in the domain and matrix phases.

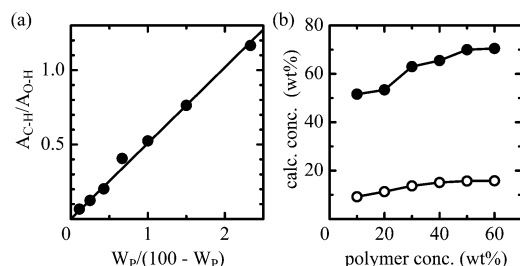


**Figure 2.** (a) Integrated intensity ratio of the  $\nu(C-H)$  band of PiPA to the  $\nu(O-H)$  band of water  $A_{C-H}/A_{O-H}$  measured at 20 °C are plotted against  $W_p/(100 - W_p)$ . (b) Calculated concentrations of PiPA in the polymer-rich phase (●) and the solvent-rich phase (○) at 40 °C are plotted against overall polymer concentration (wt %).

the  $\nu(C-H)$ ,  $\nu(O-H)$ , and  $\nu(C-D)$  bands, respectively. Although hydrogen–deuterium exchange occurs between OD of 2-propanol- $d_8$ , H<sub>2</sub>O, and the amide N–H of PiPA, its effect on the Raman spectra and properties of the solution is relatively small because the number of labile deuterium is about 3% of total labile hydrogen. Parts b and c of Figure 4 show changes in the concentration of PiPA and 2-propanol- $d_8$  estimated from the ratios  $A_{C-H}/A_{O-H}$  and  $A_{C-D}/A_{O-H}$ , respectively, in the polymer-rich and solvent-rich phases at a cooling process. The result clearly indicates that 2-propanol- $d_8$  is concentrated in the polymer-rich phase. A similar result was obtained when the PiPA/D<sub>2</sub>O/2-propanol- $d_8$  ternary mixture was used. However, methanol was not concen-

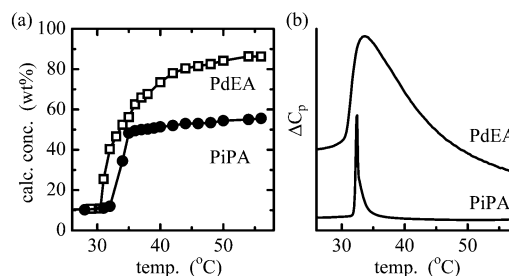


**Figure 3.** (a) Temperature dependence of the concentration of PiPA (●) and PdEA (□) in the polymer-rich phases above the LCST. Overall polymer concentration was 10 wt %. (b) DSC thermograms of the aqueous solutions of PiPA (bottom) and PdEA (top).

trated to the polymer-rich phase (data not shown), suggesting that hydrophobicity is important for the concentration.

In conclusion, the changes in polymer concentration during phase separation of aqueous polymer solutions are observed in situ by using confocal Raman microscopy. This method is suitable to determine the distribution of cosolvents and other additives such as medicines as well as polymer chains. Further study is under progress in our laboratory.

**Acknowledgment.** This work was supported by a Grant-in-Aid for Scientific Research (14550845) from Japan Society for the Promotion of Science.

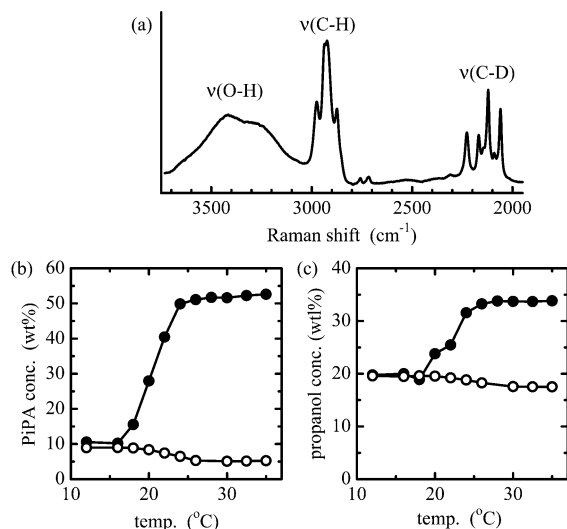


**Figure 4.** (a) Raman spectrum of the PiPA/H<sub>2</sub>O/2-propanol-*d*<sub>8</sub> mixture in the polymer-rich phase at 35 °C. (b) Calculated concentration of PiPA and (c) 2-propanol-*d*<sub>8</sub> in the polymer-rich (●) and solvent-rich (○) phases are plotted against temperature.

## References and Notes

- (1) Fujishige, S.; Kubota, K.; Ando, I. *J. Phys. Chem.* **1989**, *93*, 3311.

- (2) Tiktopulo, E. I.; Bychkova, V. E.; Rička, J.; Ptitsyn, O. B. *Macromolecules* **1994**, *27*, 2879. (b) Inomata, H.; Goto, S.; Otake, K.; Saito, S. *Langmuir* **1992**, *8*, 687. (c) Schild, H. G.; Tirrell, D. A. *J. Phys. Chem.* **1990**, *94*, 4352.
- (3) Ohta, H.; Ando, I.; Fujishige, S.; Kubota, K. *J. Polym. Sci., Polym. Phys. Ed.* **1991**, *29*, 963. (b) Tokuhiro, T.; Amiya, T.; Mamada, A.; Tanaka, T. *Macromolecules* **1991**, *24*, 2936.
- (4) Walter, R.; Rička, J.; Quillet, C.; Nyffenegger, R.; Binkert, T. *Macromolecules* **1996**, *29*, 4019. (b) Winnik, F. M. *Macromolecules* **1990**, *23*, 233.
- (5) Wang, X.; Qiu, X.; Wu, C. *Macromolecules* **1998**, *31*, 2972. (b) Meewes, M.; Rička, J.; Silva, M.; Nyffenegger, R.; Binkert, T. *Macromolecules* **1991**, *24*, 5811. (c) Kubota, K.; Fujishige, S.; Ando, I. *J. Phys. Chem.* **1990**, *94*, 5154.
- (6) Lee, L.-T.; Cabane, B. *Macromolecules* **1997**, *30*, 6559.
- (7) Maeda, Y.; Higuchi, T.; Ikeda, I. *Langmuir* **2000**, *16*, 7503.
- (8) Terada, T.; Inada, T.; Kitano, H.; Maeda, Y.; Tsukida, N. *Macromol. Chem. Phys.* **1994**, *195*, 3261. (b) Appel, R.; Xu, W.; Zerda, T. W.; Hu, Z. *Macromolecules* **1998**, *31*, 5071. (c) Appel, R.; Zerda, T.; Wang, C.; Hu, Z. *Polymer* **2001**, *42*, 1561. (d) Kato, E.; Murakami, T. *Polymer* **2002**, *43*, 5607.
- (9) Gupper, A.; Wilhelm, P.; Schmied, M.; Kazarian, S. G.; Chan, K. L. A.; Reussner, J. *Appl. Spectrosc.* **2002**, *56*, 1515.
- (10) Maeda, Y.; Nakamura, T.; Ikeda, I. *Macromolecules* **2002**, *35*, 10177.
- (11) Mizuno, K.; Ochi, T.; Shindo, Y. *J. Chem. Phys.* **1998**, *109*, 9502. (b) Gu, Y.; Kar, T.; Scheuner, S. *J. Am. Chem. Soc.* **1999**, *121*, 9411. (c) Hobza, P.; Havlas, Z. *Chem. Rev.* **2000**, *100*, 4253.

MA034311G